Astron. Astrophys. 351, 644–656 (1999)

ASTRONOMY AND ASTROPHYSICS

# Velocity variations of semiregular variables in the infrared

**T. Lebzelter**⋆

Institut für Astronomie, Universität Wien, Türkenschanzstrasse 17, 1180 Vienna, Austria

Received 10 July 1999 / Accepted 1 September 1999

**Abstract.** We obtained time series of high resolution spectra around 1.6 $\mu$m for 15 short period semiregular variables to study the velocity variations in their atmospheres with the help of second overtone vibration-rotational lines of CO. All objects of our sample clearly show velocity variations of a few km s$^{-1}$. The amplitude of the 'blue' SRVs (according to Kerschbaum & Hron 1992) is on the average a factor of two smaller than that of the 'red' SRVs. Periodicity of the variations differs from star to star. Some SRVs vary with the period listed in the General Catalogue of Variable Stars (GCVS4), others with a considerable longer period. But for all SRVs the measured velocities at 1.6 $\mu$m are over a large part of the cycle smaller than the velocities found in the literature. Different explanations of this feature are discussed. We think that the observed difference in mean velocity might be caused by a blueshift due to large convective cells on the stellar surface.

**Key words:** stars: variables: general – stars: AGB and post-AGB – stars: atmospheres

## 1. Introduction

Variability is a primary characteristic of stars on the asymptotic giant branch. Brightness variations occur on time scales of 30 to 1000 days and these variables are therefore called long period variables. They can be further divided into miras and semiregular variables (SRVs) depending on the amplitude and regularity of the variation.

The variability is thought to be caused by a pulsation of the atmosphere. This pulsation has been successfully monitored in miras and a few long period semiregular variables with the help of high excitation $\Delta$v=2 and $\Delta$v=3 vibration rotation lines of CO by Hinkle and collaborators (see Lebzelter et al. 1999 for a complete list of references). These lines are located in the near infrared (2.3 and 1.6 $\mu$m, respectively), where the flux maximum of cool stars coincides with an opacity minimum allowing a much deeper look into the atmosphere than in the visual region.

The result of these investigations was that all miras exhibit similar velocity variations clearly correlated with the visual light cycle. The velocity curve is s-shaped and discontinuous with line doubling around maximum phase. This is an indicator of a shock front running through the atmosphere. The amplitude of the velocity variations is similar for all miras and lies between 20 and 30 km s$^{-1}$. On the other hand, the few SRVs investigated up to now show much smaller velocity amplitudes. The irregularity known from the light curves of SRVs is also found in the shape of the velocity curve. While the variations are quite periodic for miras, non-periodic behavior seems common among the SRVs (Hinkle et al. 1997). The characteristics of the variations are independent from metallicity or chemistry both for miras and SRVs.

The pulsational properties revealed by the monitoring of near infrared CO lines provide an essential input for the understanding and modelling of the atmospheres of long period variables. The pulsation leads to a largely extended atmosphere and is an important factor for the extensive mass loss observed in these stars.

The properties of the SRVs and the relation of this class of variables to the miras are still a matter of debate. Kerschbaum & Hron (1992) showed that miras and SRVs have similar number densities and scale heights (except the short period miras and the 'blue' SRVs), suggesting that both groups of variables are in a similar evolutionary status. At a given period SRVs are cooler and more luminous than miras[1], suggesting a higher mode of pulsation of the SRVs. However, on average SRVs are hotter than miras and show a less expressed mass loss.

Miras form a much more homogeneous group of objects in several aspects (visual amplitude, velocity amplitude, period and periodicity) than SRVs do. The detection of a set of parameters typical for miras was supported by the much richer observational data base existing for this group of variables. For SRVs data are still lacking, also concerning velocity variations of these objects. In this paper we present new results in the latter field for a sample of short period SRVs with periods $\lesssim$ 150 days.

*Send offprint requests to*: lebzelter@astro.univie.ac.at

⋆ Visiting Astronomer, Kitt Peak National Observatory, National Optical Astronomy Observatories, which is operated by the Association of Universities for Research in Astronomy, Inc. (AURA) under cooperative agreement with the National Science Foundation.

[1] i.e. a SRV has a lower mean density than a mira with the same period, if we assume a similar mass for both kinds of objects.

In a forthcoming paper (Lebzelter, Kiss & Hinkle, in preparation) we will compare the velocity variations of semiregular variables with the light change in the visual. A third paper will deal with the relation between the velocity variations and other stellar properties for the whole sample of long period variables (Lebzelter, Hinkle & Hron, in preparation).

## 2. Observations and data reduction

Time series of infrared spectra have been obtained for a sample of 15 short period SRVs with the Coudé Feed Telescope at Kitt Peak National Observatory using the NICMASS camera as detector. This spectrograph-detector combination is described in Joyce et al. (1998). The setup was chosen to achieve a resolution of 44000. At this resolution the wavelength range covered with NICMASS is rather small, only about 40 Å. Observations were done in two wavelength ranges with central wavelength at 16412 Å (wavelength region 1) and 16461 Å (wavelength region 2), respectively. In these wavelength ranges vibration-rotational lines of CO 7-4 dominate the spectrum, including the band head at 1.64 $\mu$m (wavelength region 1). Fig. 1 illustrates the typical spectral features observed in the two wavelength regions. Lines of similar transition are found in both ranges, therefore we do not expect a significant difference in the velocity behavior between them. The selection of the wavelength range was further limited by the response curve of the blocking filter necessary to limit the background radiation of the spectrograph.

Observations were obtained in March (four runs), May (one run) and June 1995 (one run) and in March 1996 (two runs). Each run consisted typically out of 2 to 3 observing nights with a switch in central wavelength from one range to the other between them. Telluric lines from the spectra of A-type stars were used for wavelength calibration as the chosen wavelength range did not cover enough comparison lines from the calibrations lamps available. The stars in our sample were selected both on their infrared brightness and to sample the period range between 30 and 150 days. Only oxygen rich stars of spectral type M were included. The stars of our sample are listed in Table 1 with some of their fundamental properties. Typically, the stars were observed once each night (see last column of Table 1).

From the results found for the velocity variations from miras and long period SRVs we expected variations with only a few km s$^{-1}$ amplitude (Hinkle et al. 1997). Therefore a high accuracy in the determination of the velocity was necessary. As most of the lines in the selected spectral ranges are still blended at the used resolution, we used a correlation method to determine the velocity variations between the observing nights. For the correlation we used a program written by Schultheis (1998) which is based on an earlier code by Stift (1986). Fig. 2 gives a typical resulting correlation function. The minimum is well expressed and calculated by fitting a parabola through the three points centered on the minimum. A possible influence of telluric lines has been checked and can be excluded. After correction of a detected velocity shift introduced by an instability of the mounting of the NICMASS dewar we achieved a final accuracy

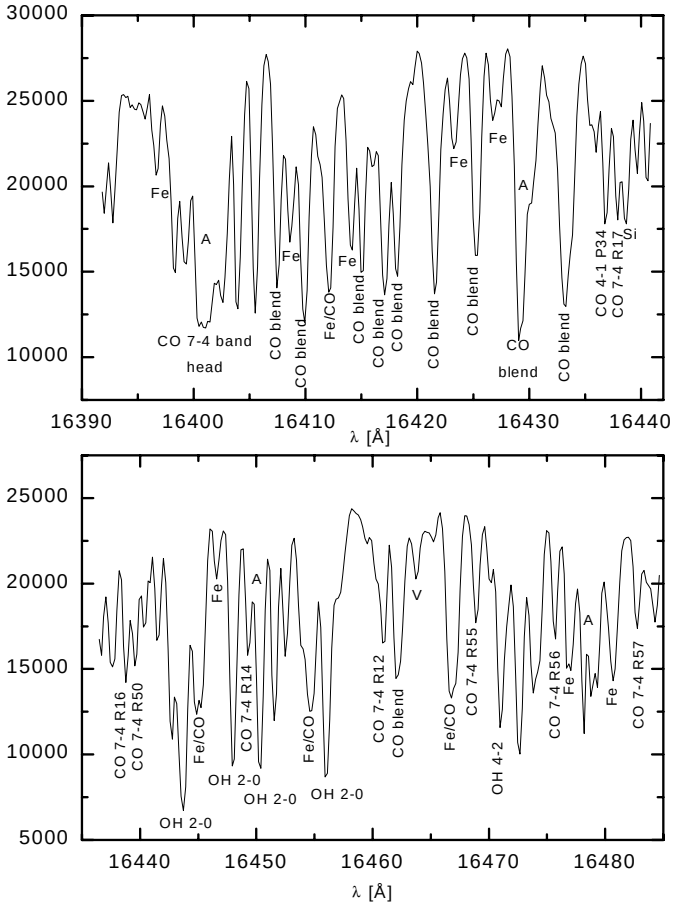


**Fig. 1.** Sample spectra of g Her for wavelength region 1 (upper panel) and wavelength region 2, respectively. Several spectral features of interest are marked. 'A' denotes telluric features. The units on the Y-axis are arbitrary.

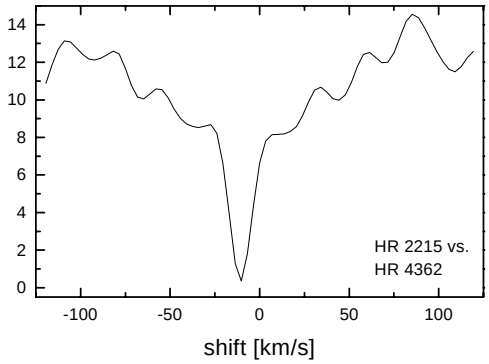


**Fig. 2.** Example of a typical correlation function used to determine the velocity shift.

of approximately 350 m s$^{-1}$ for the shift between two nights for most of the nights (for details on this correction see Lebzelter 1999a). The two wavelength regions were analyzed completely independently such that a similarity in the velocity variations could be used as a check for the reliability of the results obtained with the adopted correction method. As will be shown later, the agreement is satisfying and it can be assumed that the required

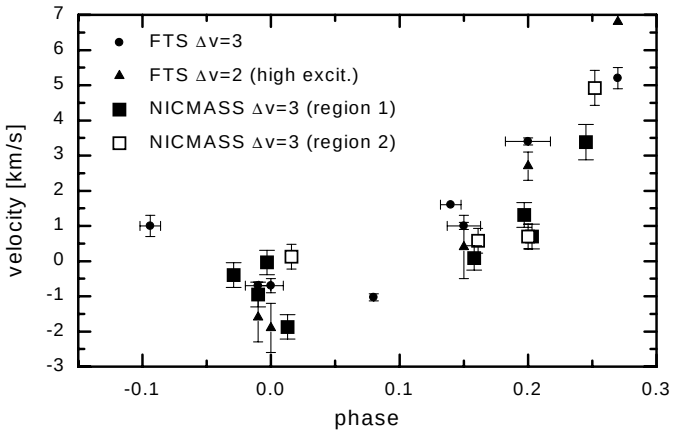


**Fig. 3.** Comparison of velocities obtained with the Coudé Feed/NICMASS with FTS velocities from Hinkle (1978) and Hinkle et al. (1984). Large symbols mark Coudé Feed velocities, small symbols FTS velocities from $\Delta$v=3 and high excitation $\Delta$v=2 CO lines. See text for more details. In the case of line doubling (FTS) only the smaller velocity component has been plotted. The error bars in phase of some of the FTS measurements are due to the fact that Hinkle (1978) gave only velocities averaged from several spectra obtained within a few days.

accuracy could be reached. A further check of the reduction applied was possible by the comparison of velocity variations from spectra of R Leo, additionally obtained in each night, with published results for this star (Hinkle 1978, Hinkle et al. 1984). A comparison of the results can be found in Fig. 3. The FTS results both for $\Delta$v=3 and for high excitation $\Delta$v=2 CO lines are plotted with small symbols, while our Coudé Feed/NICMASS velocities are plotted with large filled or open boxes for wavelength region 1 and 2, respectively. The absolute velocity for wavelength region 1 has been derived as described in Sect. 3.2. As for wavelength region 2 no absolute velocity calibration was available, we calculated them with the assumption that R Leo had the same velocity in wavelength region 2 at JD 2450174 as in wavelength region 1 at JD 2450175. It has to be stressed that, as this assumption is rather arbitrary, the *absolute* velocities of region 2 shown in Fig. 3 are no measured results (only the velocity *shifts* were measured). They were only calculated to allow an easy comparison with region 1 and the FTS velocities. Typical error bars have been used for the Coudé Feed data. Note, that the FTS velocities have been obtained about 20 years (i.e. more than 20 light cycles of R Leo) earlier than the NICMASS velocities. Taking into account the well known cycle to cycle variations in the velocitiy curves of miras (e.g. Hinkle et al. 1997) the agreement is satisfying.

It was originally planned to derive not only velocity shifts but absolute velocities for each observation. However, the stars we wanted to use as velocity references (the irregular variables UW Lyn, $\mu$ Gem and CF Boo) turned out to be not stable enough in velocity either. K-giants could not be used as their spectra were not similar enough to the M-stars of our sample for a satisfying use of the correlation method. Therefore, in Sect. 3.1 we will present only velocity shifts relative to the last two observing nights of our data set (March 1996). Sect. 3.2 will report on an estimate of the absolute velocities with the help of a contemporaneous FTS observation of three stars in our sample.

## 3. Results

### *3.1. Velocity variations*

The two wavelength regions were analyzed separately. Each region had a different reference point as observations of one night were done in only one wavelength range. Both reference points were set to a velocity equal to zero. This causes a velocity shift between the resulting velocity curves of the two regions, which depends on the variability of the object between the two reference points. However, in most cases the difference in velocity between the two reference points was found to be small compared to the total velocity variations. Still we note that for a large fraction of the stars in the sample wavelength region 2 gives slightly higher velocity values than region 1. It is most likely that an undetected small shift in the wavelength calibration of the reference night relative to the reference night of region 1 is responsible for this difference. As the velocity curves of both regions show a similar shape, it can be excluded that such a wavelength shift has any importance in the other observing nights. Visual phase information was available for some objects from parallel observations by the AAVSO or from later data obtained by the author with an automatic telescope (APT, the telescope and the observing program are described in Strassmeier et al. 1997 and Lebzelter 1999b, respectively, the results will be presented elsewhere). One well defined light maximum or minimum within the time spanned by our observations was determined and used to set the zero point of the phase. From this zero point the phases of all observations were calculated. However, SRVs can show significant cycle to cycle variations both in period lengths as well as in the shape of the light curve. This makes a continuous calculation of phases difficult. For this investigation the phases were calculated using the mean (GCVS4) period. Therefore it has to be kept in mind that due to this property of semiregular variations a calculated maximum phase does not have to be in agreement with an observed maximum. This has to be considered when discussing periodic and non periodic variations. Where no phase information was available the first observing night (JD 2449785) was taken as phase 0.

#### 3.1.1. Individual velocity curves

The velocity variations will be discussed star by star starting with the objects with the shortest periods. The velocity curves can be found in Figs. 4 to 18. The typical uncertainties of the velocity measurements of each night are plotted as error bars. The phase coverage of the radial velocity measurements allows in some cases only the estimation of a lower limit to the amplitude. The period listed in each figure caption is the one from GCVS4 (also listed in Table 1).

**Table 1.** Properties of the sample stars. Data are from the General Catalogue of Variable Stars (Kholopov et al. 1985–88, GCVS4). Column 7 lists the SRV subtype according to the new classification scheme by Kerschbaum & Hron (1992, 1994). The last column list the number of nights each star was observed for this investigation.

| Object name | IRAS name | Variability type | Spectral type | Period [d] | Vis.Ampl. [mag] | SRV type according to KH | Number of observations |
|---|---|---|---|---|---|---|---|
| $o^1$ Ori | 04497+1410 | SRb | M3 | 30 | 0.2 | blue | 11 |
| BC CMi | 07494+0324 | SRb | M5 | 35 | 0.3 | blue | 12 |
| RR UMi | 14567+6607 | SRb | M5 | 43 | 0.2 | blue | 18 |
| TU CVn | 12526+4728 | SRb | M5 | 50 | 1.1 | blue | 16 |
| BQ Gem | 07104+1614 | SRb | M4 | 50 | 0.4 | blue | 12 |
| ER Vir | 14039-1358 | SRb | M4 | 55 | 0.2 | blue | 18 |
| RR CrB | 15396+3842 | SRb | M5 | 61 | 1.7 | blue | 15 |
| TX Dra | 16342+6034 | SRb | M4e–M5e | 78 | 2.3 | red | 17 |
| g Her | 16269+4159 | SRb | M6 | 89 | 2.0 | red | 18 |
| RY CrB | 16211+3057 | SRb | M10 | 90 | 1.2 | red | 16 |
| X Her | 16011+4722 | SRb | M6e | 95 | 1.1 | red | 18 |
| TT Dra | 17120+5755 | SRb | M6 | 107 | 2.0 | red | 15 |
| OP Her | 17553+4521 | SRb | M5 | 120 | 0.9 | red? | 15 |
| RV Boo | 14371+3245 | SRb | M5e–M7e | 137 | 1.9 | red | 17 |
| ST Her | 15492+4837 | SRb | M6–7 | 148 | 1.5 | red | 17 |

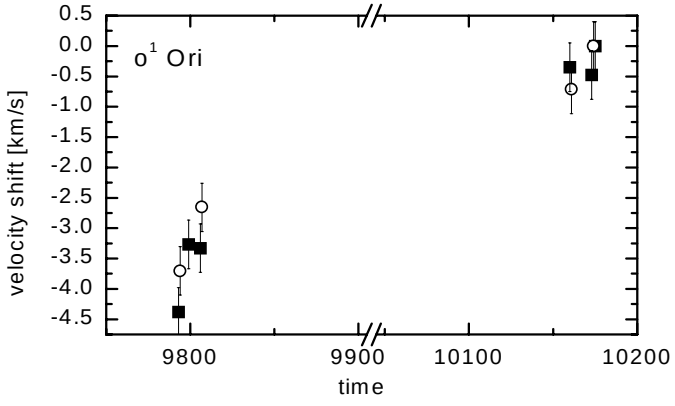


**Fig. 4.** Velocity variations of $o^1$ Ori (P=30$^d$) versus time. Solid boxes denote measurements from wavelength region 1, while open circles mark data from wavelength region 2. Time is JD minus 2440000.

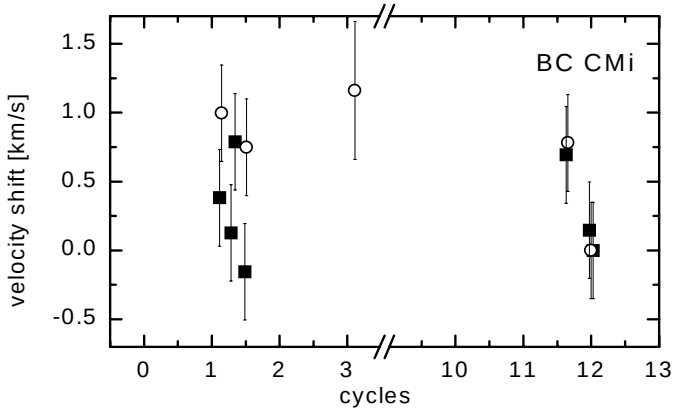


**Fig. 5.** Velocity variations of BC CMi (P=35$^d$). Same symbols as in Fig. 4.

**$o^1$ Ori** (Fig. 4) is a double star with a white dwarf companion. Parameters describing the orbital motion are missing in the literature. The evolutionary status of this object was discussed in detail by Jorissen & Mayor (1992). In Fig. 4 we plotted the velocity shifts against Julian Date as on the one hand the period of the intrinsic variations is not well known (GCVS4), and on the other hand the observed variations might be dominated by the orbital motion. Variations in both wavelength ranges agree satisfactorily. The maximum velocity difference observed within anyone of the two ranges is approximately 4.5 km s$^{-1}$. Brown et al. (1990) reported several velocity measurements at 7500 Å over a time span of 330 days. The maximum difference found from these velocities is 2.2 km s$^{-1}$. The available data are not sufficient to derive the intrinsic velocity variation. A hand-drawn interpolation of the velocity curve suggests that we probably see a combination of orbital motion (or a secondary period) and variations on a short time scale, e.g. the GCVS4 period.

**BC CMi** shows only very small variations of about 1 km s$^{-1}$ (Fig. 5). It is not clear whether these variations are related to the photometric period. Variations on a significantly longer time scale cannot be excluded, but are also not really supported by the data. Due to the very short period of the star, about 10 cycles (period = 35 days) lie between the 1995 and the 1996 observations. This makes a combination of the results quite difficult. After all, for that small velocity changes, the typical error of the velocities of about 350 m s$^{-1}$ strongly limits the reliability of the results. The position of the star in the sky did not allow to observe this object in May and June 1995.

**RR UMi** is the second double star of our sample. Its orbital elements are well known so that we used the orbital period to calculate the phase (Fig. 6). Our observations cover about half a cycle. In Fig. 6 we additionally plotted the expected velocity variation due to the orbital motion of RR UMi calculated from the parameters given by Batten & Fletcher (1986). For ease

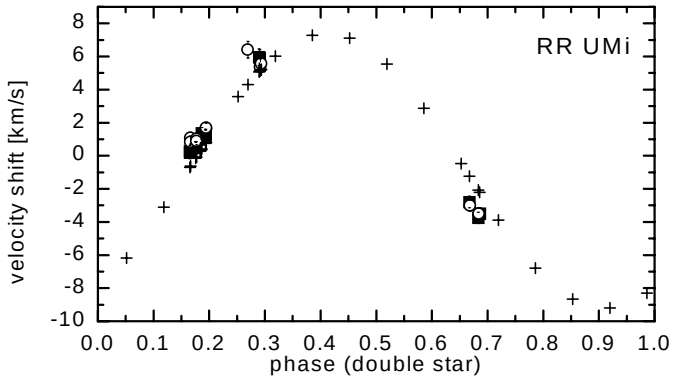


**Fig. 6.** Velocity variations of RR UMi (P=43$^d$). Same symbols as in Fig. 4. The double star period (748.9$^d$) has been used to calculate the phase. Expected velocity variations due to orbital motion are marked with crosses (see text).

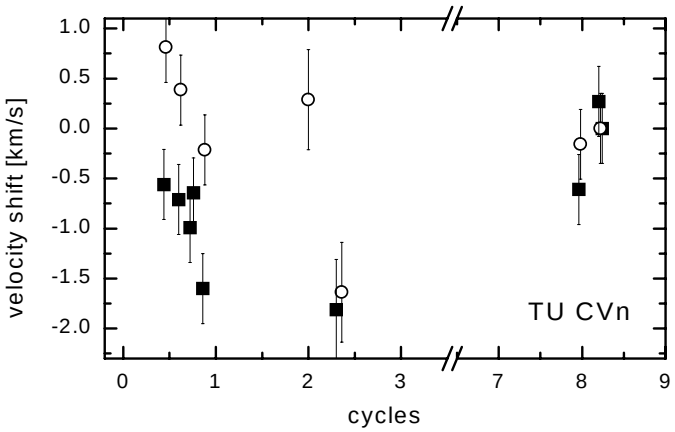


**Fig. 7.** Velocity variations of TU CVn (P=50$^d$). Same symbols as in Fig. 4.

of comparison, the Coudé Feed velocities have been shifted to overlap with the (orbital) velocity curve from Batten & Fletcher. Note, that at this point we measured only velocity *shifts*. It can be seen that the variations we observe from the CO lines are mainly due to the orbital motion. This star has been observed two times in some nights. The variations found within one night are very small.

The light variations of **TU CVn** do not follow the mean period accurately. For phase estimation we used a maximum derived from our own light curve data at JD 2450420. The velocity variations are plotted in Fig. 7. Variations of about 3 km s$^{-1}$ are indicated in both wavelength regions. Plotting all observations between phase 0 and 1 did not lead to useful results. The irregularities in period found from the visual light curves seem to be represented in the velocity variations, too. Phase estimation will therefore not be very reliable.

Only a few data points were obtained for **BQ Gem**. The resulting velocity variations are plotted in Fig. 8. An estimate of the amplitude gives 1.5 km s$^{-1}$. The lower panel of Fig. 8 gives the velocity variations versus phase. Periodic changes are possible.

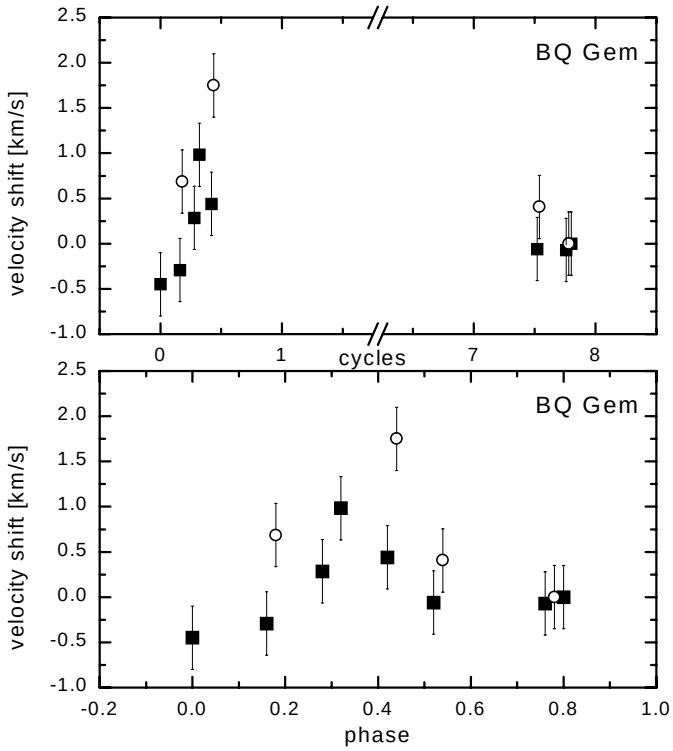


**Fig. 8.** Velocity variations of BQ Gem (P=50$^d$). The lower panel shows the variations versus estimated phase. Same symbols as in Fig. 4.

No phase information was available for **ER Vir** (Fig. 9). For the observing runs in 1995 an untypically large shift in velocity is observed between the two wavelength regions. The origin of this is not clear. Reducing all data to one period (lower panel of Fig. 9) shows no expressed periodicity. The amplitude is estimated to be 2 to 2.5 km s$^{-1}$. The scatter is quite large and as a comparison with the light curve was not possible, a definite description of a possible regularity cannot be given.

Velocity variations found for **RR CrB** are plotted in Fig. 10. Plotting the data simply in time (bottom axis in Fig. 10) suggests variations with a period several times the period found in the GCVS4. A secondary period of 377 days has been found by Houk (1963) and the corresponding phases (relative to the first observation) can be seen in the top axis of Fig. 10. This period leads to a quite reasonable result. The long period case would lead to a velocity amplitude of the order of 3 to 3.5 km s$^{-1}$. However, the velocity curve shows variability on a shorter timescale with a a smaller amplitude of about 1 km s$^{-1}$, too. A combination of the GCVS4 (short) period option with the long period of Houk seems likely. The long period behavior might also be due to an orbital motion, but no indications exist that this object is a binary.

The observed velocity changes of **TX Dra** suggest a possible periodic behavior with the period known from visual light changes (Fig. 11). Phase estimation is provided by AAVSO data. The velocity curve looks continuous and similar to the observations found for RU Cyg (Hinkle et al. 1997). The amplitude is about 5 km s$^{-1}$. Good agreement is found between the vari-

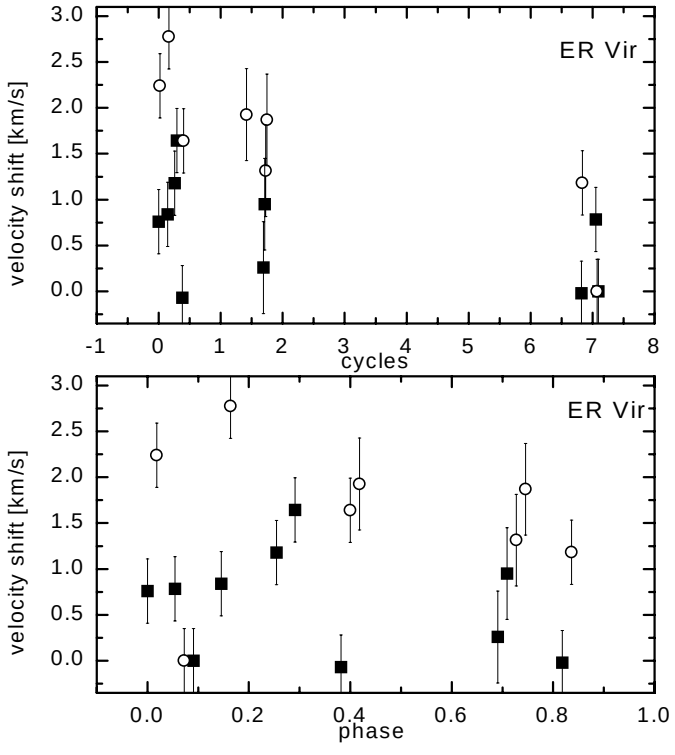


**Fig. 9.** Velocity variations of ER Vir (P=55$^d$). The lower panel shows the variations versus estimated phase. Same symbols as in Fig. 4.

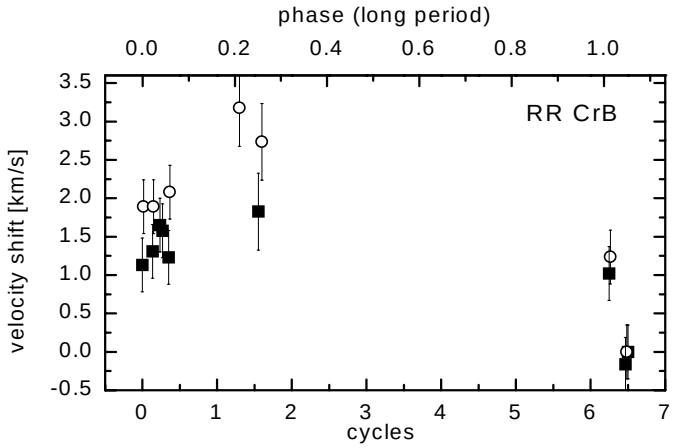


**Fig. 10.** Velocity variations of RR CrB (P=61$^d$). Same symbols as in Fig. 4. The bottom axis gives the cycles calculated with the GCVS4 (short) period. The top axis gives the phase calculated from the long period of 377$^d$ (see text).

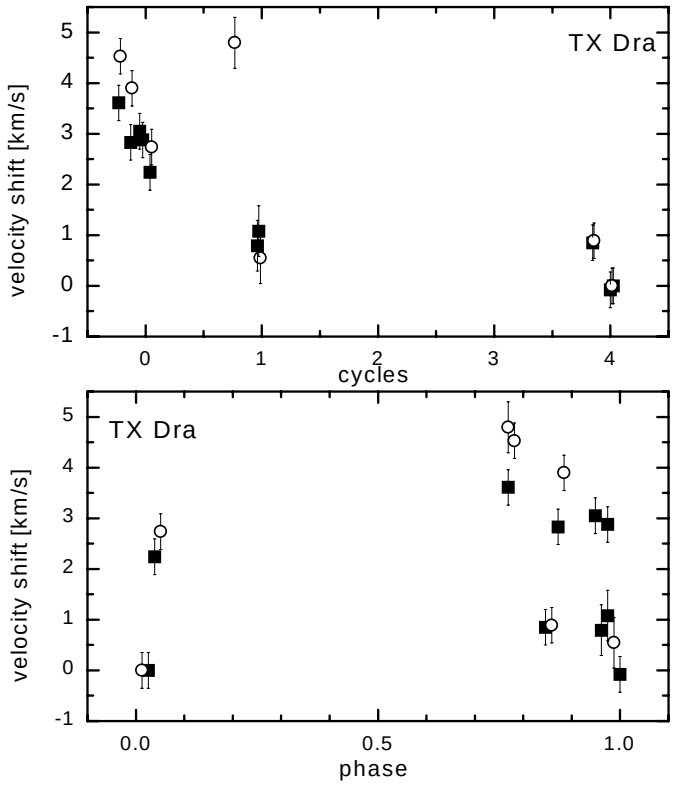


**Fig. 11.** Velocity variations of TX Dra (P=78$^d$). Same symbols as in Fig. 4. The lower panel shows the velocity shift versus phase.

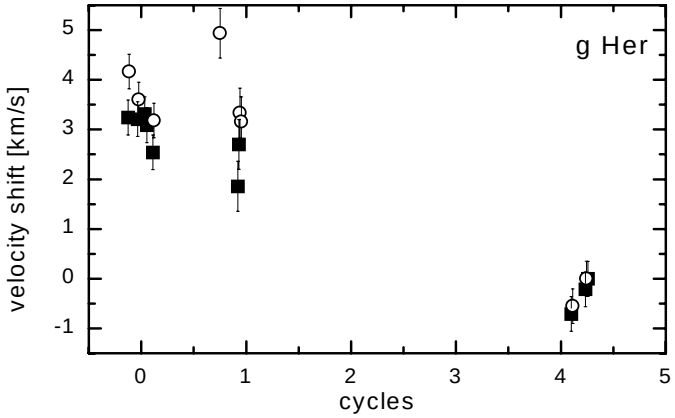


**Fig. 12.** Velocity variations of g Her (P=89$^d$). Same symbols as in Fig. 4.

ous wavelength regions. Kiss et al. (1999) have found two more periods in the light changes of TX Dra of 137 and 706 days, respectively. There is no indication for a 137$^d$ period in the velocity variations. To check a possible influence of the longer period considerably longer time series of velocity measurements would be necessary. Kiss et al. expect a mode switch in that object around 1999-2000. It would be interesting to monitor the behavior of the velocity variations close to this mode switch.

**g Her** shows velocity variations with an amplitude of approximately 3.5 to 4 km s$^{-1}$ (Fig. 12). The variations do not follow the mean period, but seem to represent the semiregular changes of the light curve. Comparable trends can be seen in both wavelength regions. A secondary period as indicated by long time AAVSO observations (889 days, Mattei et al. 1997) cannot be excluded, but time coverage of velocity data is not good enough to detect this secondary period.

The velocity variations of **RY CrB** (Fig. 13) would be one of the largest found within our sample of short period SRVs, if we assume that these variations are due to the stellar pulsation. However, variations clearly do not follow the period known from the visual light curve. Two scenarios could explain the

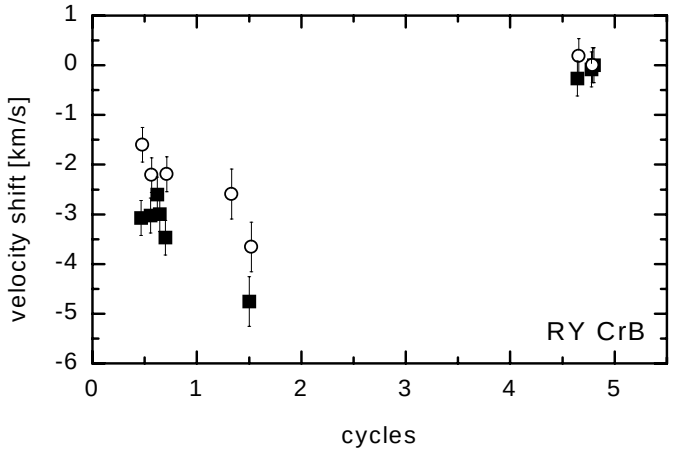


**Fig. 13.** Velocity variations of RY CrB (P=90$^d$). Same symbols as in Fig. 4.

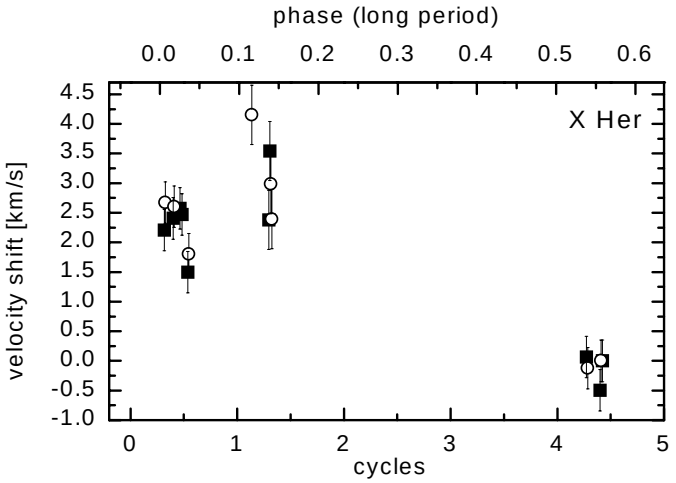


**Fig. 14.** Velocity variations of X Her (P=95$^d$). Same symbols as in Fig. 4. Top axis corresponds to the secondary period of 746 days.

outstanding behavior of this star. First, it could be an unknown double star. Then these variations would be dominated by the orbital motion as evidenced for RR UMi. This hypothesis is supported by Hipparcos measurements. The Hipparcos Catalogue (ESA 1997) lists RY CrB as variability induced mover (VIM), which is a suspected double star system with the brighter component being variable. Further observations of this object would be necessary to verify this hypothesis. The other possibility is a longer "secondary" period, which is the dominant one but has not been observed up to now. Whatever explanation is correct, small, short time scale variations of radial velocity are also observed, so that a description of the behavior has to include both long and short period variation. The velocity curve suggests that the longer period is at least 5 times the GCVS4 period (i.e. more than 450$^d$).

Variations of **X Her** seem to agree roughly with a period half as long as the one from the light variations. Phases were estimated from our own light curve data. AAVSO data had too much scatter for a clearly defined maximum. From our data a velocity amplitude of at least 1.5 to 3 km s$^{-1}$ can be estimated (Fig. 14). A secondary, significantly longer period of 746$^d$ has been found by Houk (1963) and is illustrated in the top axis of Fig. 14. The available data strongly suggest that the velocity of this star varies on both time scales. The total amplitude of the long period variation cannot be determined but seems to be about 4.5 km s$^{-1}$.

For **TT Dra** we used a rough phase estimation from AAVSO data. The velocity shifts exhibit a nicely shaped variation (Fig. 15, upper panel), that seems to be reasonably periodic (Fig. 15, lower panel). The amplitude is about 3.5 km s$^{-1}$, and the variations agree well in both wavelength regions. It cannot be decided whether the velocity curve is continuous and comparable to RU Cyg (see Fig. 6 of Hinkle et al. 1997) or discontinuous and thus more like the variations known from miras. This is mainly indicated by the data point close to phase 0 in Fig. 15, lower panel, but the quality of the spectrum at this point is low. However, no line doubling was visible and data

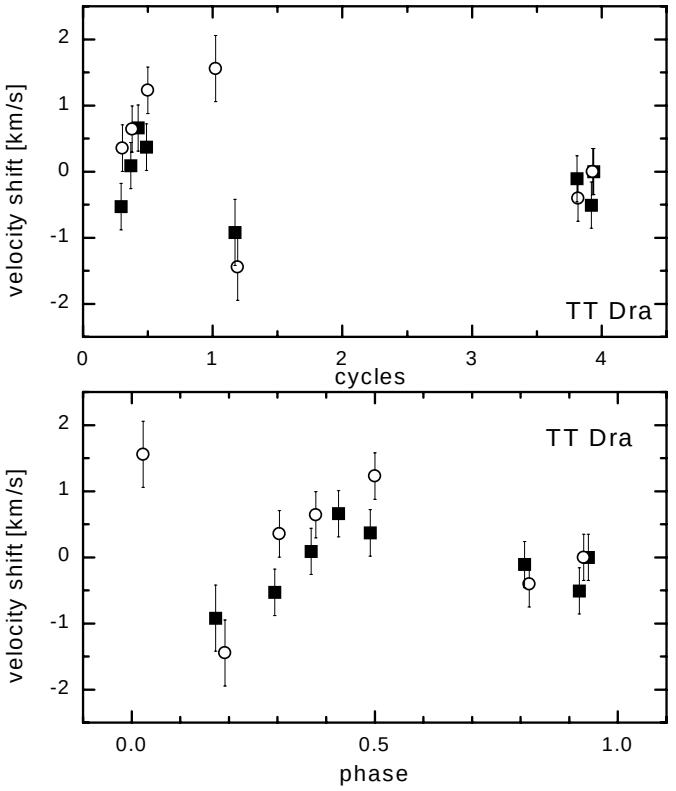


**Fig. 15.** Velocity variations of TT Dra (P=107$^d$). Same symbols as in Fig. 4. The upper panel shows the variations plotted versus time. The lower panel shows the variations with phase.

from only two cycles were combined here. This object would be highly interesting for further monitoring.

Velocity variations of **OP Her** are plotted in Fig. 16. The velocity amplitude is approximately 2.5 km s$^{-1}$. Agreement between the two wavelength regions is similar to other objects of the sample, but the star could not be observed in as many nights as the other stars of the sample, therefore the coverage of the variations is not as good. Variations seem to be somehow cyclic,

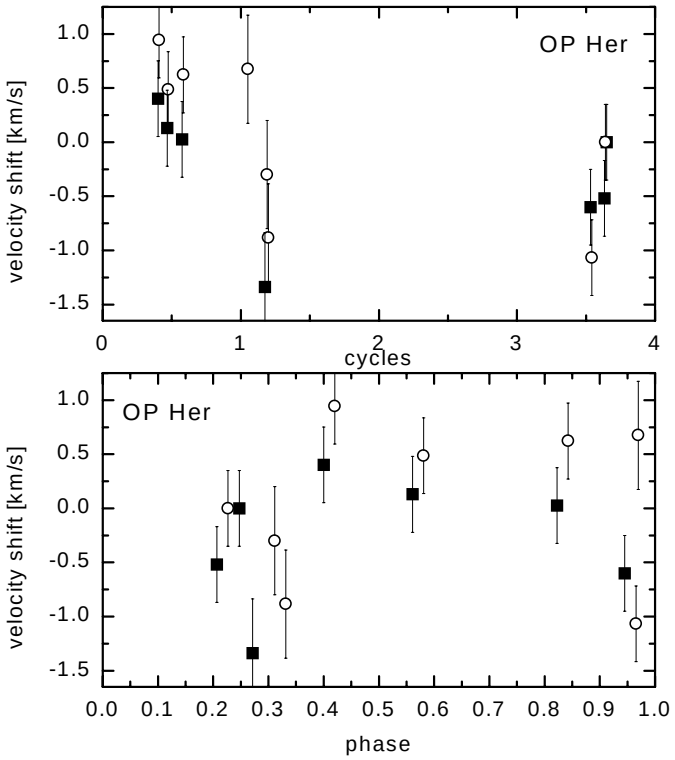


**Fig. 16.** Velocity variations of OP Her (P=120$^d$). In the upper panel the phase is calculated with the GCVS4 period of 120$^d$, in the lower panel a modified period of 50$^d$ (as suggested by recent photometric observations) is used. Same symbols as in Fig. 4.

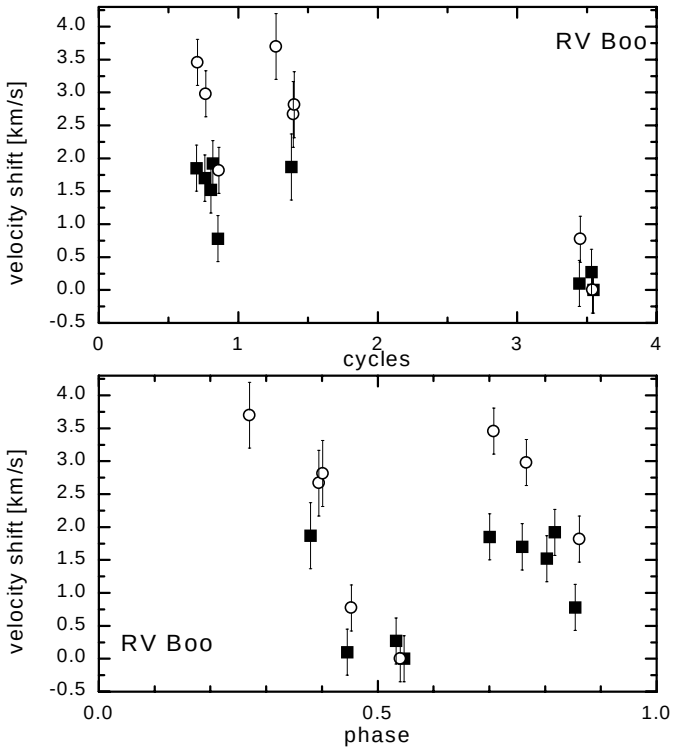


**Fig. 17.** Velocity variations of RV Boo (P=137$^d$). Same symbols as in Fig. 4. The upper panel shows the variations plotted versus time. The lower panel shows the variations with phase (GCVS4 period).

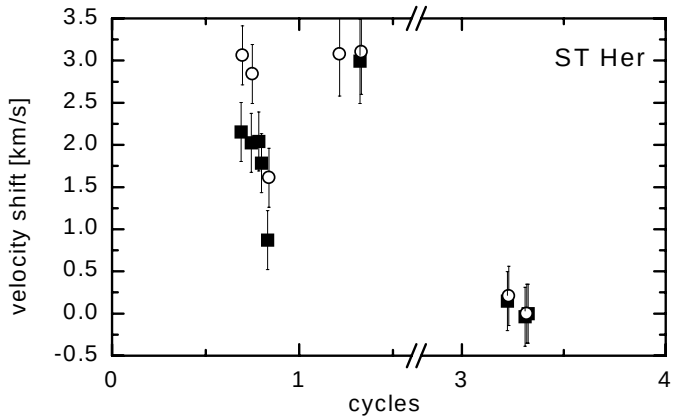


**Fig. 18.** Velocity variations of ST Her (P=148$^d$). Same symbols as in Fig. 4.

but may not actually follow the known period. APT observations of this object suggest variations on a significantly shorter timescale of about 50 days. Using 50$^d$ instead of 120$^d$ seems to fit the observed velocity variations quite good (Fig. 16, lower panel). More (accurate) light curve data are needed to check which one of the two periods is more compatible with the light variations.

**RV Boo** displays a very interesting variation (Fig. 17). Plotting all data into one cycle (lower panel of Fig. 17) the velocity seems to vary quite regularly with a period clearly shorter than the one listed in the GCVS4. Simple analysis of the velocity curve gives a period with 92 or 122 days as the best fit. As three cycles are combined, variations with this shorter period seem to be a regular behavior of the star. It is not clear, whether the period from the visual light variations is different from the one indicated by the velocity variations. A simple explaination might also be that the GCVS period is wrong, i.e. the situation would be probably comparable to that of OP Her. The velocity amplitude of the star is about 3 km s$^{-1}$.

Finally, the object with the longest period in our sample, **ST Her**, belongs to those short period SRVs where we could follow a well expressed velocity variation in our data in agreement with the visual period (Fig. 18). Phase data are from AAVSO. A velocity minimum is clearly defined around maximum phase. Due to the semiregular behavior visible in the star's light curve it is not surprising that the data observed two cycles later are shifted in phase. The amplitude is about 3 km s$^{-1}$.

### 3.1.2. 'Blue' and 'red' SRVs

From infrared and visual photometry, Kerschbaum & Hron (1992, 1994) concluded that the semiregular type SRa is not a distinct class of variables but a mixture of mira and SRb classes. They established a new classification scheme dividing the semiregular variables into 'blue' and 'red' SRVs. Including also the velocity data from the SRVs published in Hinkle et

al. (1997) we find that the 'red' SRVs have a mean amplitude which is approximately a factor of two larger than the mean amplitude of the 'blue' SRVs. The star W Hya, which has the largest velocity amplitude of all SRVs monitored, has been excluded from this calculation as its variability type is uncertain. In the light of this comparison the amplitude of TU CVn, classified as 'blue' SRV, is untypically large.

### *3.2. Absolute velocities of the CO lines*

In principle one might suppose that an absolute center of mass velocity for the objects of our sample could be obtained as a mean velocity from the different measurements. All data presented up to now in this paper are velocity *shifts* relative to a reference observation. Taking into account the observed amplitude of the velocity variations we can compute a velocity of each object in the reference night if we know the center of mass velocity of at least one object and assume that the center of mass velocity is reached at half the velocity amplitude as it is suggested from velocity curves of miras.

However, the whole method is unusable due to the probable incorrectness of the last assumption. The velocity curves of W Cyg and RU Cyg derived from FTS data (Hinkle et al. 1997) indicated already that the velocity of the high excitation CO lines does not necessarily reach the center of mass velocity at any time.

#### 3.2.1. g Her – and a problem

In the light of the problem described above and the lack of reliable standard stars we had to find an independent velocity measurement of at least one object at the time the Coudé Feed spectra were obtained. Fortunately, an FTS spectrum ($\Delta$v=2 high exc. CO lines) of g Her has been obtained by Ken Hinkle at the 4 m Mayall telescope (KPNO) in the night immediately before one of the observing nights at the Coudé Feed (JD 2449793) and kindly provided to the author. It is known from mira variables that the high excitation $\Delta$v=2 lines and the second overtone lines of CO show the same velocity behavior. We can now compare the FTS velocity of g Her (Table 2) to the variations observed in the Coudé Feed spectra. As a first assumption we propose that the velocity did not change significantly between the two nights. Although the monitored velocity variations indicate that a change between two nights is quite probable, a different starting point does not seem possible. However, the difference between two nights is typically not larger than 300 m s$^{-1}$. In the Coudé Feed velocity curve for g Her the relevant data point represents a velocity shifted from the velocity maximum observed in wavelength region 1 by only 0.1 km s$^{-1}$. We can therefore assume that the FTS (absolute) velocity represents almost the maximum velocity observed for the high excitation $\Delta$v=2 CO lines or the $\Delta$v=3 CO lines, respectively. On the other hand, the FTS velocity is about 0.4 km s$^{-1}$ less than the center of mass velocity derived from circumstellar CO radio emission. Taking into account all uncertainties in the Coudé Feed (wavelength region 1), the FTS and the radio velocity we find that the center of mass velocity is hardly reached by the observed Coudé Feed velocities at any phase. The amplitude in wavelength region 2 is a little bit larger but still a significant asymmetry between outflow and infall remains. Unfortunately it is not clear whether we really strongly underestimate the amplitude in region 1 or not.

#### 3.2.2. Other objects

What can be done to get more insight into this question, is to measure the velocity of each object in our sample in the night JD 2449793 and then derive the velocity range for each object. Under the assumption that the velocity of g Her in that night is equal to the FTS velocity we correlated all stars of that night with g Her. Additional correlation was done with the secondary standards UW Lyn, ST Her and $\mu$ Gem. The selection of these objects was made deliberately. These three stars cover most of the range of radial velocities of the members of our sample. As a result, for almost every star we have such a template that the resulting pixel shift in the correlation is small, which reduces the error of the velocity derived by correlation. Furthermore, two of the objects were observed in the beginning of the night, ST Her and g Her after midnight. The scatter of the velocities derived from these four objects could therefore help to estimate the influence of the absolute pixel shift on the accuracy of the derived velocities. The current velocity of these stars was determined by correlation with g Her.

The results of this correlation are given in Table 3. For each star the velocity given is the average of the velocities relative to the four standard objects with the exceptions of a few objects where the velocity shift was too large for some of the templates and therefore gave no reliable result. The standard deviation derived from the four templates is given and indicates the error of the correlation method. The agreement between the values from the four templates is impressively good.

We calculated from this reference point the minimum and maximum velocity measured in wavelength region 1. A comparison with velocity data from the literature is given in Table 3. For a number of stars of our sample we measured the radial velocity with the Coudé Feed in the *blue* region around 4300 Å. These measurements were obtained on March 30 1995 (JD 2449806). The accuracy achieved is about 1.5 km s$^{-1}$. If there was a large difference between the literature value and our *blue* velocity, the latter one is listed in Table 3, which is indicated by "LZ" in Column 7 of that table. We found differences between the literature values and our data of up to 10 km s$^{-1}$.

Some objects show very large differences between the literature value and the derived velocity on JD 2449793. These cases can be explained quite well either as double stars (RR UMi and o$^1$ Ori), suspected double stars (RY CrB) or large amplitude variables (R Leo).

A closer look at the velocity differences listed in Table 3 (Columns 8 and 9) shows that for several objects the maximum Coudé Feed velocity is less than the literature value. The difference, however, is always below 1 km s$^{-1}$. This is also valid for those objects that exceeded at some phase the velocity listed in

**Table 2.** Radial velocities derived from FTS spectra of g Her, X Her and RR UMi obtained on March 14, 1995

| GCVS name | rv low exc. CO lines | number of lines used | rv high exc. CO lines | number of lines used |
|---|---|---|---|---|
| g Her | 2.18±0.32 | 6 | 0.93±0.17 | 5 |
| X Her | −88.77±0.39 | 12 | −89.62±0.22 | 4 |
| RR UMi | 7.03±0.48 | 10 | 7.21±0.22 | 4 |

**Table 3.** Attempt to derive absolute velocities for the SRVs observed with NICMASS for JD 2449793. Velocities have been calculated using the correlation technique as described in the text. The template for the correlation was g Her adopting an FTS velocity. ST Her, UW Lyn and $\mu$ Gem were used as secondary templates. The second column gives the mean velocity derived from the four standards with the standard deviation listed in Column 3. Columns 4 and 5 give the respective observed maximum and minimum velocity calculated from the relative RV variations in wavelength region 1; the latter were determined by using the velocity shifts relative to JD 2449793. Column 6 gives the velocity value found in the literature. Column 7 lists the source of the literature value (TCO...thermal CO (Kerschbaum & Olofsson 1999), GC...General Catalogue of Stellar Radial Velocities (Wilson 1953), LZ...see text). Column 8 and 9 give the difference between literature value and the maximum and mean observed Coudé Feed velocities, respectively. All velocities are heliocentric and in km s$^{-1}$. Stars are sorted by constellation. Only one template could be used for X Her due to the star's high system velocity.

| Object | velocity JD 2449793 | $\sigma$(vel) | maximum velocity | minimum velocity | literature value | Reference | $v_{max}-$Lit | $v_{mean}-$Lit |
|---|---|---|---|---|---|---|---|---|
| Boo CF | −15.8 | 0.16 | −14.9 | −16.3 | −15.5 | LZ | 0.6 | −0.1 |
| Boo RV | −6.7 | 0.07 | −6.5 | −8.4 | −6.2 | TCO | −0.3 | −1.3 |
| CMi BC | −66.4 | 0.10 | −66 | −67 | −66.2 | LZ | 0.2 | −0.3 |
| CVn TU | −20 | 0.10 | −19 | −21.1 | −19.7 | LZ | 0.7 | −0.4 |
| CrB RR | −60.7 | 0.10 | −60.1 | −62.1 | −60.3 | LZ | 0.2 | −0.8 |
| CrB RY | 18.9 | 0.03 | 21.9 | 17.1 | 28 | Feast et al. (1972) | −6.1 | −8.5 |
| Dra TT | −13.5 | 0.14 | −12.9 | −14.5 | −12 | LZ | −0.9 | −1.7 |
| Dra TX | 45.7 | 0.06 | 46.5 | 42.8 | 46.4 | LZ | −0.1 | −1.8 |
| Gem $\mu$ | 53.4 | 0.15 | 54 | 52.8 | 54.8 | GC | −0.8 | −1.4 |
| Gem BQ | −11.1 | 0.07 | −9.8 | −11.2 | −9.2 | GC | −0.6 | −1.3 |
| Her g | 0.9 | 0.11 | 1 | −3.1 | 1.4 | TCO | −0.4 | −2.5 |
| Her OP | 9.1 | 0.04 | 9.4 | 7.7 | 10 | LZ | −0.5 | −1.5 |
| Her ST | −23.1 | 0.01 | −22.1 | −25.1 | −22 | TCO | −0.1 | −1.6 |
| Her X | −89.2 | – | −88.1 | −92.1 | −90 | TCO | 1.9 | −0.1 |
| Leo R | −0.4 | 0.13 | 3.4 | −1.9 | 7.5 | TCO | −4.1 | −6.8 |
| Lyn UW | 9.2 | 0.07 | 10.5 | 9.2 | 11.3 | GC | −0.8 | −1.5 |
| Ori o$^1$ | −10.9 | 0.04 | −6.5 | −10.9 | −7.9 | Evans (1967) | 1.4 | −0.8 |
| UMi RR | 7.3 | 0.04 | 12.8 | 3.1 | 6.2 | Batten & Fletcher (1986) | 6.6 | 1.75 |
| Vir ER | 7.7 | 0.12 | 8.5 | 6.8 | 8.2 | GC | 0.3 | −0.6 |

the literature, which means that the literature value is very close to the maximum value observed. The only exception is X Her, which is probably due to a secondary period.

The difference between literature value and Coudé Feed velocities gets even more obvious when comparing the *mean* Coudé Feed velocity (wavelength region 1) instead of the maximum velocity. The results are listed in Table 3 (Column 9). All differences are negative, on the average about 1.2 km s$^{-1}$ (ignoring the objects with large velocity differences noted before). In fact, this means that there is a significant asymmetry between the outflow and infall relative to the center of mass velocity (if the latter is represented by the literature values) in all objects of our sample. This common behavior suggests that it is not due to chance. Possible explanations will be discussed in Sect. 4.2

## 4. Discussion

### *4.1. Velocity variations*

The short period SRVs fit well into the picture indicated by the variables with longer periods. Typical amplitudes for these stars are found to be about 2 to 4 km s$^{-1}$. In most cases the two wavelength regions investigated agree in their amplitude and shape of the variations. Some stars seem to vary with the period of the visual brightness variations, others behave irregularly or may follow a different period. Obviously, variations do not always follow the same period for every cycle making a merging of observations from different cycles almost impossible. Representative for this behavior are the variations observed in g Her or TU CVn.

The third type of variability found within the small sample observed is visible in TT Dra, TX Dra and BQ Gem. OP Her and RV Boo might be further candidates for this type, but the uncertainty in period actually does not allow a definite conclusion. Both objects show variations that might indicate a period somewhat smaller than the GCVS4 period. The variations in these stars look very similar to the variations found for RU Cyg, but both their amplitudes and periods are a bit smaller. It cannot be excluded that such variations could be found also in other stars, but they are masked by bad phase coverage or uncertainties in the period. As mentioned above, TT Dra might even behave similar to the miras but with a much smaller velocity amplitude.

Furthermore, two stars of our sample, RR CrB and X Her, show variations that might be connected both to short period and long period variations. For both stars a secondary period is indicated from the light curve. In two more objects, g Her and RY CrB, such a "double variation" in the radial velocity data may be visible as well. This result implies that the secondary, longer periods could be very important for the understanding of the short period semiregular variables. However, for RY CrB the variations might be due to orbital motion around a companion star.

### *4.2. Absolute velocities*

The observed difference between center of mass velocities and velocities derived from the CO $\Delta$v=3 lines might be due to one or more of the following reasons:

#### 4.2.1. Technical reasons

- The same explanation is valid that was found possible for g Her, i.e. wavelength region 1 would generally underestimate the velocity amplitude. In fact, inspection of the velocity curves of both regions shows that this might be true for several objects. However, it is not found in all stars and the difference in amplitude beween the two wavelength regions is not in all cases large enough to explain the observed discrepancy in general.
- The assumption is wrong that the velocity of g Her is almost constant between the two nights: Fortunately, FTS spectra of two more stars have been obtained in that night (see Table 2). The velocity difference between the calculated Coudé Feed value and the FTS value for RR UMi is 0.1 km s$^{-1}$ and for X Her 0.4 km s$^{-1}$. Both differences are almost within the uncertainties of the FTS/Coudé-Feed velocities, but even if the difference would indicate an error in the FTS velocity of g Her, it is too small to shift the detected asymmetry sufficiently.
- One aspect that cannot be excluded as it has not been tested up to now is that a velocity difference occurs between the 2.2 $\mu$m region (FTS-spectra) and the 1.6 $\mu$m region (Coudé-Feed). Such an assumption is not supported by the results from miras where the velocities from the high excitation CO $1^{st}$ overtone lines in the K-band and the CO $2^{nd}$ overtone lines show the same velocity behavior[2]. However, the possibility exists that semiregular variables behave differently. If so, one can think of two possibilities: Either the velocity variation at 2.2 $\mu$m is shifted in phase relative to the variation at 1.6 $\mu$m, so that a velocity difference occurs. Or the velocity amplitude at 2.2 $\mu$m is significantly larger than at 1.6 $\mu$m. The disadvantage of both explanations is the fact that such a behavior is not observed in miras. These are thought to be even more extended than SRVs, and a main condition to achieve such a difference will be a very large extension of the object. Tuthill et al. (1998) find that for W Hya, a semiregular variable, radii at 1.65 and 2.26 $\mu$ are very similar (see Hinkle et al. 1997 for the velocity curve of W Hya). Furthermore, typical indicators of shock fronts (emission lines, line doubling), that would allow a large velocity difference on a small scale, were not found in the SRVs of our sample. Although this explanation cannot be ruled out without a detailed modelling of AGB-star atmospheres, it seems rather unlikely.

#### 4.2.2. Literature values

- The literature values are inaccurate: This would be quite probable in some cases as already mentioned in the previous section. Still, incorrect values should not be systematically biased towards larger velocities. Furthermore, obvious cases of wrong velocities in the literature have been corrected by our own 'blue' spectra.
- The literature values are correct but do not represent the center of mass velocity: Most of the literature data (and also our own data indicated by LZ in Table 3) are based on visual/photographic spectra. From different investigations (e.g. Hinkle & Barnes 1979) it is known that for miras the velocity derived from blue atomic lines is not identical with the center of mass velocity, but is red-shifted. In our case the literature values are also *red-shifted* relative to the velocities derived from the CO lines. On the other hand, system velocities derived from radio CO lines, which exist for a small part of the sample, have been used in the list of literature data in Table 3. They exhibit the same direction of the velocity shift as the 'blue' velocities. But it has to be noted that the velocities from radio CO lines, although in principle very accurate indicators of the center of mass velocity, display a significant scatter of up to a few km s$^{-1}$ within the literature. Furthermore, radio CO line profiles were found to be asymmetric in some cases. In these cases deriving a center of mass velocity from these lines becomes quite difficult.

[2] In this context we want to note that Hinkle et al. (1982) found a difference in velocity between the 2.2 $\mu$m and 1.6 $\mu$m region of more than 3 km s$^{-1}$ for single observations of the mira $\chi$ Cyg, but averaged over the whole light cycle no difference was found between the two wavelength regions. Due to the similar results for three different stars (g Her, X Her and RR UMi) it is not very likely that individual differences as found by Hinkle et al. could solve our observed discrepancy.

#### 4.2.3. Additional velocity components

As the above listed attempts could not or at least not completely explain the observed difference, it has to be assumed that we see outflowing matter over most of the cycle. It is quite unlikely that no inward movement of material happens.

- The long period option: It might also be the case that we do not see these objects at their center of mass velocity because we did not observe long enough. Secondary periods of SRVs appeared already several times in this paper. If they are of the order of 1000 days, our sampling might be not sufficient. This interpretation was already suggested for W Cyg (Hinkle et al. 1997). On the other hand, such a long 'main' period of pulsation, that is not or only marginally expressed in the light changes, seems quite unlikely. Such a long time variation could also be due to unknown companions. However, this is indicated only for a few stars of our sample. Furthermore it does not allow to explain a systematic difference between the observed velocity and the literature value, for one would expect a scatter around the center of mass velocity in that case.
- Temperature effect: Maybe we see only one component because of the difference in temperature between the hot outflowing material and the cool infalling matter, so that the latter might not be visible. This would be in agreement with the fact that line doubling is never observed in these stars. On the other hand, we have to note that the lines are visible throughout the whole light cycle. We found no spectrum where the lines actually vanished which would then correspond to a phase of 'pure' infall.
- Granulation: A temperature effect as described before could get important, if we see an overlap of pulsation and convection. A velocity asymmetry could originate from large convective cells at the surface that are thought to be present in these stars (Schwarzschild 1975, Weigelt et al. 1998). The phenomenon of an overall blue shift of the measured velocity by convection effects is well known from the sun, resulting from the interplay between granular intensity and velocity fields. The general case of granulation in stars has been discussed by Dravins (1987), but investigations on cool and extended objects are lacking. However, only model calculation could proove whether the size of the velocity shift can be explained in this way, which is beyond the scope of this paper. We just want to mention that the spectral features investigated in this paper are almost exclusively line blends or even molecular band heads. Therefore an analysis of the line profiles that would lead to information on the origin of the observed variations is not feasible. Compared with the other possibilities discussed convection seems to be a realistic possibility to explain the observed phenomenon. In this context it is interesting to note that two of the three irregular variables in Table 3, $\mu$ Gem and UW Lyn, clearly show the same direction of the velocity shift. Therefore to have a common explanation for all stars of our sample a mechanism that can be found in every cool and extended atmosphere, like convection, seems preferable.

Observational material presented in this paper as well as in the literature does neither exist for a sample sufficiently large nor is it accurate enough both in velocity and in the coverage of the whole light cycle to allow any final conclusions at the moment.

Different answers might be true for different objects. As this velocity difference was found for some long period SRVs (Hinkle et al. 1997), too, it might be a common feature for semiregular variables. In that case, however, a common explanation for all SRVs would be more likely.

## 5. Conclusions and outlook

Velocity variations were clearly detected in all short period semiregular variables of our sample. These variations can reach an amplitude of up to $4\,\mathrm{km\,s^{-1}}$. Periodicity is detected in several cases, but did not always follow the GCVS4 period from the visual light change. Some objects seem even to vary on two time scales. Following the classification by Kerschbaum & Hron (1992) we find that 'red' SRVs on average have a larger velocity amplitude than the 'blue' SRVs. Combining these results with previous investigations on SRVs with longer periods we conclude that this group of variables follows a rough period-velocity amplitude relation, with long period objects having larger velocity amplitudes. This relation will be discussed in more detail in a forthcoming paper. Like in Hinkle et al. (1997) we note that semiregular and mira variables can be clearly separated on their velocity amplitude.

The difference between center of mass velocities and the measurements presented in this paper remains puzzling. Any attempt to derive accurate center of mass velocities at high accuracy from the velocity variations at 1.6 $\mu$m is problematic unless the origin of this velocity shift has been understood. Not enough data are available, both at 1.6 $\mu$m and in the radio regime, to derive any kind of statistical correction factor, if this were possible at all.

Data for a significantly larger sample would be necessary to investigate both, the velocity displacement and the possibility of subtypes among the SRVs according to the regularity, periodicity and shape of their velocity variations. Such an extension would have to include both long period and short period SRVs. However, obtaining time series of these variables consumes enormous amounts of telescope time. Especially the scheduling of such an observing program is difficult. While data for long period objects like miras, with only small changes in the behavior from cycle to cycle, can be collected over a long time span requiring only a small number of observing nights in each season, short period objects like the SRVs would need continuous observations over a long time to be able to establish systematics in the velocity changes.

Spectroscopy of the investigated CO lines with a significantly higher spectral resolution would be necessary for a detailed investigation of the profiles of individual lines to derive further conclusions on possible surface structures influencing the observed velocity variations. This could lead to an improved understanding of the nature of semiregular variables in general.

An interesting aspect would be a comparison with an extended sample of CO radio velocities for these SRVs, which is unfortunately not yet available in the literature. Finally, new concepts to understand this behavior will only be provided by improved models of the stellar atmosphere in AGB stars.

*Acknowledgements.* This work was supported by Austrian Science Fund Project S7308. The author wishes to thank K. Hinkle, R. Joyce and D. Willmart for support with the observations and fruitful discussions on the data reduction. Special thanks to Ken for obtaining the FTS spectra and help with the reduction of these data. Further thanks go to J. Hron, H.M. Maitzen and M.J. Stift as well as the referee for helpful comments on the manuscript. This research made use of the SIMBAD database operated by CDS in Strasbourg, France. In this research, we have used, and acknowledge with thanks, data from the AAVSO International Database, based on observations submitted to the AAVSO by variable star observers worldwide.

## References

Batten A.H., Fletcher J.M., 1986, PASP 98, 647
Brown J.A., Smith V.V., Lambert D.L., et al., 1990, AJ 99, 1930
Dravins D., 1987, A&A 172, 200
Evans D.S., 1967, In: Batten A.H., Heard J.F. (eds.) IAU Symp. 30, Determination of radial velocities and their application. Academic Press, New York, p. 57
ESA, 1997, The Hipparcos and Tycho Catalogues. ESA-SP 1200
Feast M.W., Wooley R., Yilmaz N., 1972, MNRAS 158, 23
Hinkle K.H., 1978, ApJ 220, 210
Hinkle K.H., Barnes T.G., 1979, ApJ 234, 548
Hinkle K.H., Hall D.N.B., Ridgway S.T., 1982, ApJ 252, 697
Hinkle K.H., Scharlach W.W.G., Hall D.N.B., 1984, ApJS 56, 1
Hinkle K.H., Lebzelter T., Scharlach W.W.G., 1997, AJ 114, 2686
Houk N., 1963, AJ 68, 253
Jorissen A., Mayor M., 1992, A&A 260, 115
Joyce R.R., Hinkle K.H., Meyer M.R., Skrutskie M.F., 1998, Proc. SPIE 3354, in press
Kerschbaum F., Hron J., 1992, A&A 263, 97
Kerschbaum F., Hron J., 1994, A&AS 106, 397
Kerschbaum F., Olofsson H., 1999, A&AS, in press
Kholopov P.N., Samus N.N., Frolov M.S., et al., 1985-88, General Catalogue of Variable Stars. $4^{th}$ edition, Nauka Publishing House, Moscow (GCVS4)
Kiss L.L., Szatmáry K., Cadmus R.R., Mattei J.A., 1999, A&A 346, 542
Lebzelter T., 1999a, Ph.D. Thesis, Univ. of Vienna
Lebzelter T., 1999b, A&A 346, 537
Lebzelter T., Hinkle K.H., Hron J., 1999, A&A 341, 224
Mattei J.A., Foster G., Hurwitz L.A., et al., 1997, In: Battrick B. (ed.), Hipparcos - Venice '97, ESA SP-402, 269
Schultheis M., 1998, Ph.D. Thesis, University of Vienna
Schwarzschild M., 1975, ApJ 195, 137
Stift M.J., 1986, MNRAS 219, 203
Strassmeier K.G., Boyd L.J., Epand D.H., Granzer Th., 1997, PASP 109, 697
Tuthill P., Monnier J., Danchi W., 1998, In: Bradley P.A., Guzik J.A. (eds.) A Half Century of Stellar Pulsation Interpretations. ASP Conf. Ser. 135, p. 322
Weigelt G., Balega Y., Blöcker T., et al., 1998, A&A 333, L51
Wilson R.E., 1953, General Catalogue of Stellar Radial Velocities. Carnegie Inst., Washington D.C., Publ. 601